An Overview of Multi-Dimensional RF Signal Processing for Array Receivers

Arjuna Madanayake
Electrical and Computer Engineering
The University of Akron
Akron, Ohio, 44325-3904
Email: arjuna@uakron.edu

Chamith Wijenayake
Electrical Engineering and Telecom
University of New South Wales
Sydney NSW 2052, Australia
Email: c.wijenayake@unsw.edu.au

Leonid Belostotski and Len T. Bruton
Electrical and Computer Engineering
University of Calgary
Alberta T2N 1N4, Canada
Email: {lbelosto,bruton}@ucalgary.ca

***Abstract*—In this review paper, recent advancements in multidimensional (MD) spatio-temporal signal processing for highly-directional radio frequency (RF) antenna array based receivers are discussed. MD network-resonant beamforming filters having infinite impulse response (IIR) and recursive spatio-temporal signal flow graphs are reviewed. The concept of MD network-resonant pre-filtering is described as a modification to existing phased/timed array beamforming back-ends to achieve improved side-lobe performance in the array pattern, leading to better interference rejection capabilities. Both digital and analog signal processing models are described in terms of their system transfer functions and signal flow graphs. Example MD frequency response and RF antenna array pattern simulations are presented.**

***Keywords*—Multidimensional Signal Processing, Phased Arrays**

I. Introduction

Antenna array-based directional receivers are employed in a multitude of radio frequency (RF) applications ranging from electronically-scanned radar, microwave sensing, long-range detection and target tracking, source localization, radio telescope arrays and wireless communications [1]–[6]. Multi-input-multi-output (MIMO) wireless systems and cognitive radios utilize array processing to exploit spatial domain diversity, directional gain, and interference mitigation [7], [8]. Moreover, array processing algorithms and circuits have been explored towards achieving better spatial (directional) selectivity, interference rejection, multiple RF receiver beams, and computationally efficient processing architectures [3], [6], [9]. Antenna arrays lead to multi-dimensional (MD) spatio-temporal signals. Processing of wideband MD array signals at multi-GHz frequencies in the microwave and mm-wave regime require signal processing algorithms as well as RF analog and digital parallel processing circuits in order to support massive real-time data throughput. We report recent advancements in the area of MD array processing based on network-resonant filters [10] and their RF analog and digital electronic realizations.

Directional receivers have been based on the phased/timed arrays having transversal transfer functions. These are devoid of complex pole-manifolds [7], [11]. Recent research on MD filters have led to phased/timed array processors with MD network-resonant filtering algorithms having infinite impulse responses (IIRs). These modified phased/timed arrays yield improved inference rejection capabilities via significantly reduced side-lobe levels (see Fig. 1) [12]–[15].

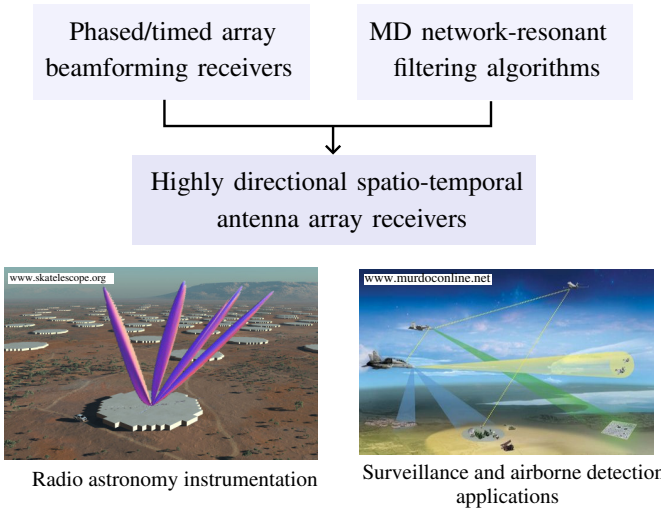

Fig. 1: Application of MD network-resonant filtering algorithms in conjunction with conventional phased/timed arrays leading to highly directional spatio-temporal array receivers having potential applications in radar and RF sensing.

II. Directional Filtering and Network Resonant MD Space-Time Filters

We focus the discussion to uniform linear arrays (ULAs) corresponding to two-dimensional (2-D) signals $w(n_x, n_{ct})$ (assuming RF-to-bits digitization at each antenna) where n_x is the antenna index and n_{ct} is the time sample index. For analog MD processing the ULA signal is $w(n_x, ct)$, where ct is the normalized space-like time variable.

To explain the beamforming operation in MD signal processing perspective, let us consider a propagation scenario, where the ULA received signal $w(n_x, n_{ct})$ consisting of uniform far-field RF plane-wave signals arriving at an angle ψ to array broadside. It is recalled the 2-D frequency spectrum of $w(n_x, n_{ct})$ has a line-shaped region of support (ROS) oriented at an angle $\theta = \tan^{-1}(\sin\psi)$ in the 2-D spatio-temporal frequency domain (ω_x, ω_{ct}) [10]. Here, ω_x and ω_{ct} are the spatial and temporal frequency variables, respectively. Selective filtering of radio waves with the direction of arrival (DOA) ψ can be achieved by having a 2-D filter with appropriately oriented beam/cone-shaped passband in the

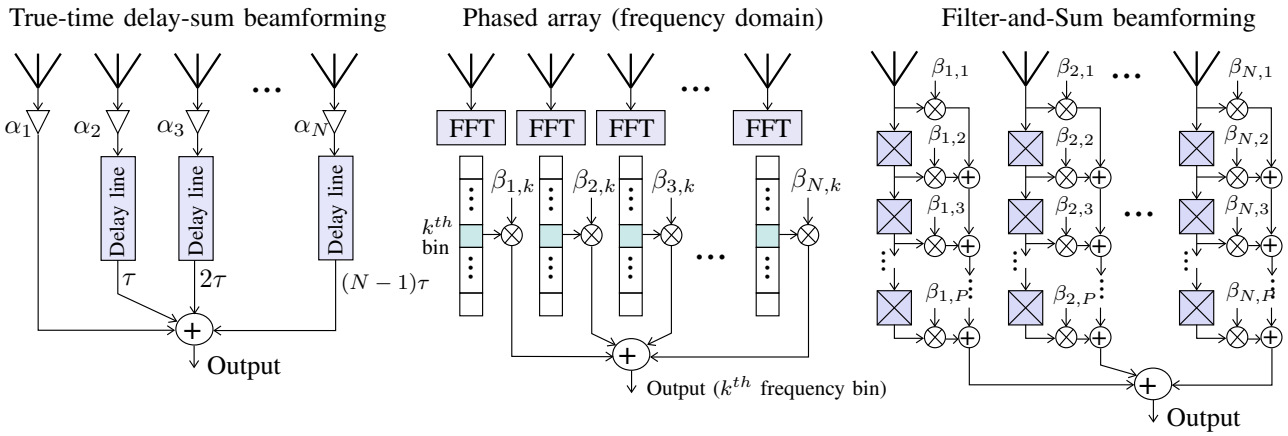

Fig. 2: Different realizations of phased/timed array directional receivers having zero-manifold only array transfer functions.

2-D frequency domain [10], [16]. In general, a beamforming algorithm (in digital domain for example) can be described by a 2-D spatio-temporal transfer function

$$T_{BF}\left(z_x, z_{ct}\right) = \frac{\sum_{p=0}^{P}\sum_{q=0}^{Q} a_{pq} z_x^{-p} z_{ct}^{-q}}{1 + \sum_{p=0}^{P}\sum_{q=0}^{Q} b_{pq} z_x^{-p} z_{ct}^{-q}} \equiv \frac{N\left(z_x, z_{ct}\right)}{D\left(z_x, z_{ct}\right)}, \quad (1)$$

where $z_x \in \mathbb{C}$ and $z_{ct} \in \mathbb{C}$ are spatial and temporal **z**-transform variables, respectively. The coefficients $a_{pq} \in \mathbb{R}$ and $b_{pq} \in \mathbb{R}$ set the passband shape, orientation, and selectivity in the 2-D frequency response function. For conventional phased/timed arrays, (1) implies a zero-manifold only array transfer function, where $D\left(z_x, z_{ct}\right) \equiv 1$. Various algorithms exist to obtain optimized array weights a_{pq} that lead to a desired array beam pattern. Fig. 2 reviews three realizations of phased/timed arrays.

The concept of MD network resonance allows the synthesis of highly selective MD denominator polynomials in the array transfer function (1) (i.e. insertion of complex pole-manifolds defined by $D\left(z_x, z_{ct}\right) = 0$) at guaranteed practical bounded-input-bounded-output (p-BIBO) stability [17]. Fig. 3(a) shows an example of a first-order 2-D inductor-resistor passive prototype network having the 2-D Laplace domain transfer function

$$H\left(s_x, s_{ct}\right) = \frac{R}{R + L_x s_x + L_{ct} s_{ct}} \quad (2)$$

where s_x and s_{ct} are the Laplace transform variables in spatial and temporal dimensions, respectively. The 2-D frequency response function corresponding to (2) $H\left(s_x = j\omega_x, s_{ct} = j\omega_{ct}\right)$ exhibits planar-resonance along a line-shaped region given by $L_x\omega_x + L_{ct}\omega_{ct} = 0$, leading to a beam-shaped filter passband as shown in Fig. 3(b). By appropriately selecting the network parameters (L_x, L_{ct}, and R) orientation and sharpness of the beam passband can be controlled. For example, by selecting $L_x = \cos\left(\tan^{-1}\left(\sin\psi\right)\right)$ and $L_{ct} = \sin\left(\tan^{-1}\left(\sin\psi\right)\right)$, an electronically steerable far-field beam pointing at an angle ψ from array broadside direction can be obtained [10]. The prototype transfer function $H\left(s_x, s_{ct}\right)$ can be used to obtain p-BIBO stable digital or analog domain array processing 2-D filters having both zero- and pole-manifolds in their transfer functions with recursive spatio-temporal signal flow graphs (SFGs).

III. Digital Array Receivers with Improved Directional Selectivity

Prototype network transfer function (2) can be used to obtain the 2-D discrete domain transfer function [18]

$$H_D\left(z_x, z_{ct}\right) = \frac{\left(1 + z_x^{-1}\right)\left(1 + z_{ct}^{-1}\right)}{1 + b_{10} z_x^{-1} + b_{01} z_{ct}^{-1} + b_{11} z_x^{-1} z_{ct}^{-1}} \quad (3)$$

where the coefficients $b_{pq} = \frac{R + (-1)^p \cos\theta + (-1)^q \sin\theta}{R + \cos\theta + \sin\theta}$ [18] with $p, q = 0, 1$ and $b_{00} = 0$ set the orientation (controlled by θ)

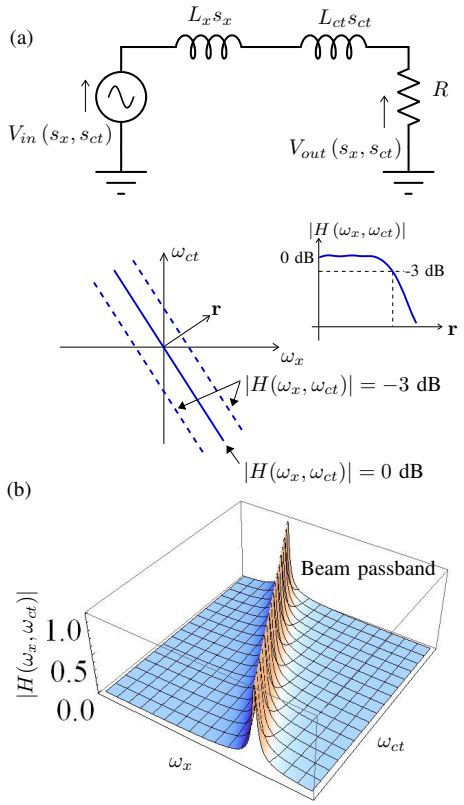

Fig. 3: (a) First order 2-D passive prototype network and (b) corresponding 2-D frequency response with the beam-shaped passband.

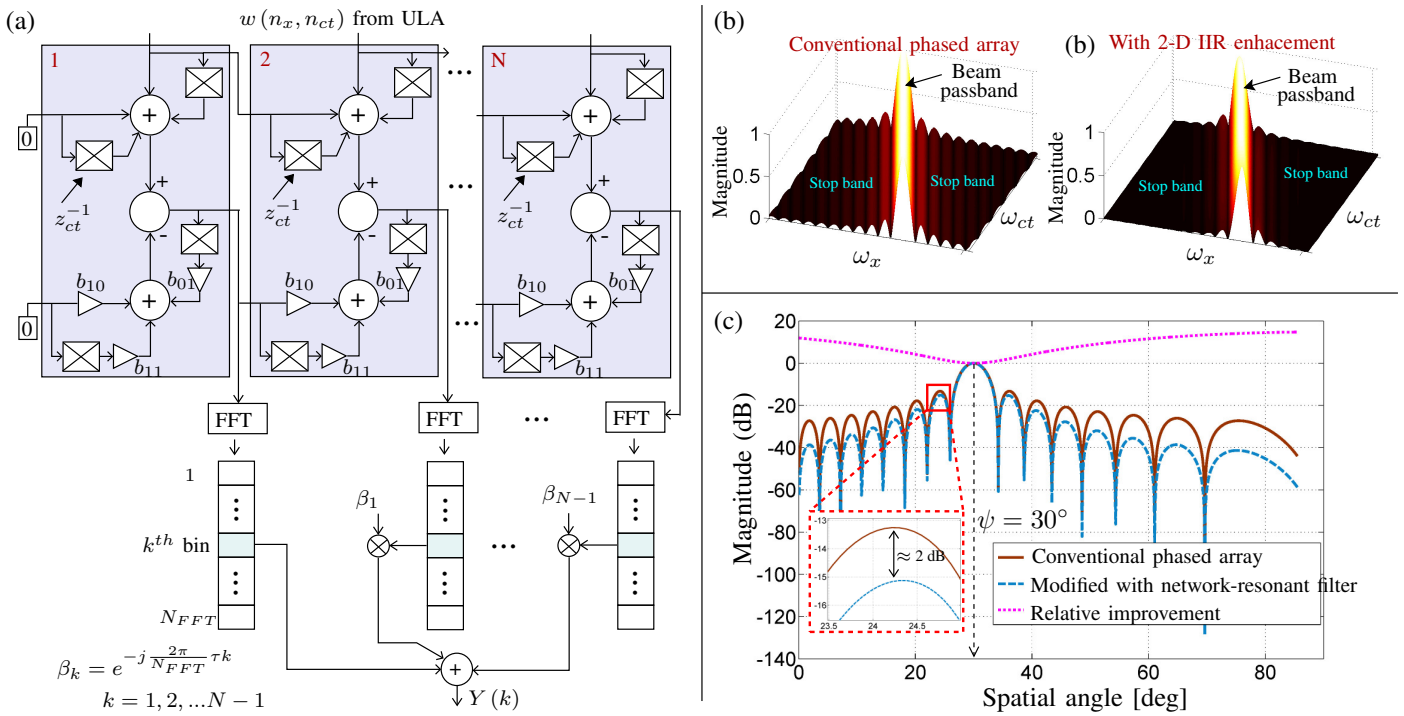

Fig. 4: (a) Signal flow graph of a ULA receiver with 2-D network-resonant digital beam filter connected to a phased array. (b) 2-D magnitude frequency response and (c) array pattern depicting the reduced side-lobe levels obtained by introducing 2-D network-resonant pre-filter.

and sharpness (controlled by R) of the beam passband. These p-BIBO stable 2-D IIR digital filters have recursive spatio-temporal SFGs described by the 2-D difference equation

$$y_1(n_x, n_{ct}) = \sum_{p=0}^{1}\sum_{q=0}^{1} w(n_x - p, n_{ct} - q) - \sum_{p=0}^{1}\sum_{q=0}^{1} b_{pq} y_1(n_x - p, n_{ct} - q), \quad (4)$$

where $w(n_x, n_{ct})$ and $y_1(n_x, n_{ct})$ are the 2-D input and output signals to the beam filter, respectively. Note that (4) implies an array processing architecture with interconnected identical processing modules as shown in Fig. 4(a). The multi-input-multi-output SFG pertaining to (4) allows us to employ the 2-D IIR digital beam filter described by (3) as a pre-filtering stage to conventional phased/timed array beamforming back-ends, thereby modifying the overall phased/timed array transfer function as [12]

$$T(z_x, z_{ct}) = \frac{1}{N}\frac{\left[\sum_{n_x=0}^{N-1} z_x^{-n_x} z_{ct}^{-\tau n_x}\right]\left(1 + z_x^{-1}\right)\left(1 + z_{ct}^{-1}\right)}{1 + b_{10}z_x^{-1} + b_{01}z_{ct}^{-1} + b_{11}z_x^{-1}z_{ct}^{-1}}. \quad (5)$$

Note that (5) contains complex pole-manifolds, which were not present in conventional phased/timed array model. Fig. 4(a) shows the SFG corresponding to (5), where introduction of the network-resonant 2-D IIR filter leads to a marginal increase in signal processing complexity with 3 additional multipliers per antenna.

Fig. 4(b) shows the 2-D magnitude frequency response corresponding to conventional phased/timed array model and following the network-resonant 2-D IIR pre-filtering. The frequency response function $T\left(z_x = e^{j\omega_x}, z_{ct} = e^{j\omega_{ct}}\right)$ shows reduced side-lobes in the stop-band region. Enhanced directional selectivity is shown in Fig. 4(c) in terms of the array pattern. The array pattern is computed by evaluating the frequency response at a given temporal frequency ω_{ct0} as a function of the spatial angle γ. That is, we evaluate (5) at $z_{ct} = e^{j\omega_{ct0}}$ and $z_x = e^{-j\omega_{ct0}\sin\gamma}$ to obtain the array pattern shown in Fig. 4(c), assuming a 64 element ULA, beam direction $\psi = 30°$ and $\omega_{ct0} = 0.5\pi$.

Unlike traditional approaches to control side-lobe levels via optimizing phased array weights (i.e. by optimizing the spatial window of the antenna array aperture), *2-D IIR network-resonant pre-filtering approach leads to significantly reduced side-lobe levels without compromising the main-beam directivity or array size.* It is quite likely that this approach is a fundamentally new contribution to the field of antenna array beamforming.

IV. Analog Array Receivers with Improved Directional Selectivity

Continuous-time domain realization of network-resonant 2-D IIR beam filters can be used in conjunction with conventional time-delay-sum beamformers to obtain antenna array analog processing back-ends having improved directivity (side-lobe performance). One possible approach of designing continuous-time domain network-resonant beam filters is to employ first-order all-pass filter based transfer function synthesis [13]. That is, by replacing unit-sampled time delays z_{ct}^{-1} in the discrete domain beam filter transfer function (3) with all-pass transfer function $\left(1 - \left(\frac{s_{ct}cT}{2}\right)\right) / \left(1 + \left(\frac{s_{ct}cT}{2}\right)\right)$ a discrete-space continuous-time (i.e. analog) 2-D transfer

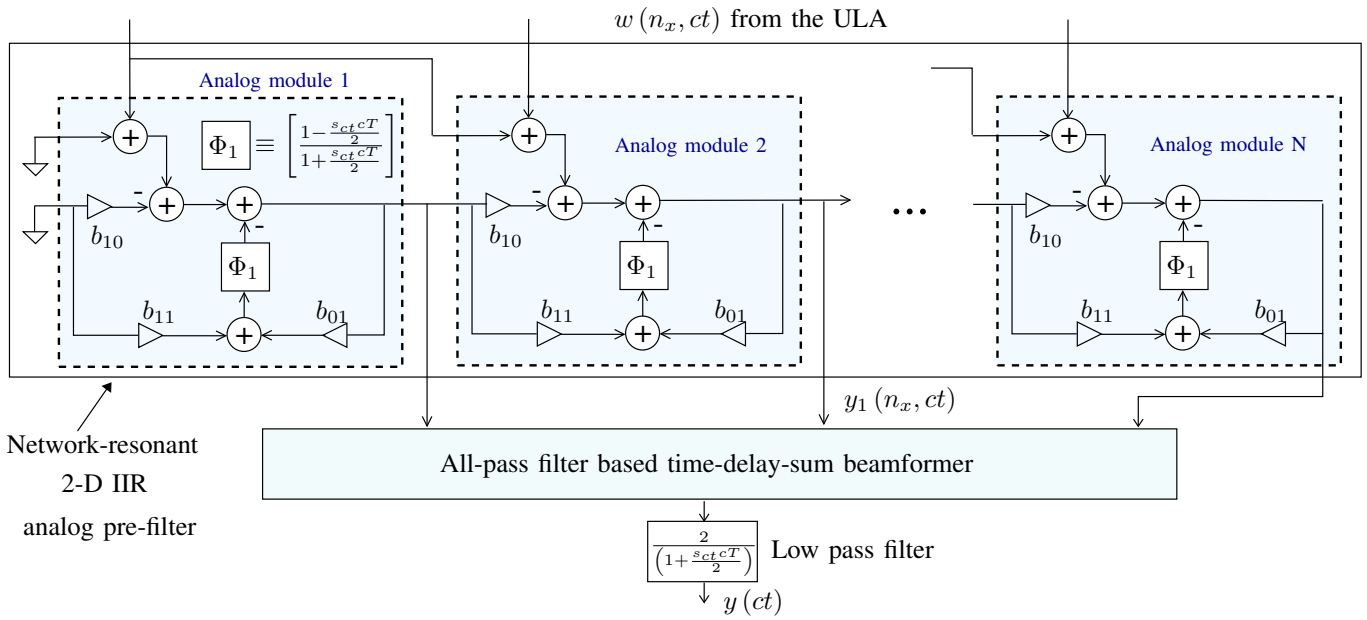

Fig. 5: System architecture of network-resonant all-pass filter-based combined 2-D IIR filter and time-delay-sum analog array processor.

function is obtained as

$$H_A(z_x, s_{ct}) = \frac{\left(1+z_x^{-1}\right)\left(\frac{2}{1+\frac{s_{ct}cT}{2}}\right)}{1+\left[b_{10}+b_{11}\left[\frac{1-\left(\frac{s_{ct}cT}{2}\right)}{1+\left(\frac{s_{ct}cT}{2}\right)}\right]\right]z_x^{-1}+b_{01}\left[\frac{1-\left(\frac{s_{ct}cT}{2}\right)}{1+\left(\frac{s_{ct}cT}{2}\right)}\right]}, \quad (6)$$

where similar to the digital case, the coefficients b_{10}, b_{01}, and b_{11} control the orientation and sharpness of the beam passband. Moreover, the use of first-order all-pass filters in place of sampled time delays removes the bilinear frequency warping effect along temporal frequencies [13].

All-pass filter based delay approximation has also been used in time-delay-sum beamforming systems (see Fig. 2), where a cascade of $M \geq 1$ all-pass filters is used to approximate element time delays required at each antenna [13]. Delay-sum beamformer 2-D transfer function for such all-pass filter based implementation is given by [13]

$$H_{DAS,A}(z_x, s_{ct}) = \frac{1}{N}\sum_{n=0}^{N-1}\alpha_n z_x^{-n}\left[\frac{1-\left(\frac{s_{ct}cT}{2M}\right)}{1+\left(\frac{s_{ct}cT}{2M}\right)}\right]^{Mn}, \quad (7)$$

where N is the ULA size, α_n defines the spatial window, and τ is the element time delay. For beam direction ψ from array broadside, $\tau = \frac{\Delta x}{c}\sin\psi$, where Δx is the ULA inter-antenna spacing. The all-pass filter cascade length M should be appropriately selected based on the required beam direction and beam pointing accuracy as described in [13].

By combining (6) and (7) a new array transfer function (8) is obtained, which now contains complex pole-manifolds, unlike the conventional time-delay-sum model described by (7). Fig. 5 shows the array processing architecture described by (8). The network-resonant 2-D analog beam filter described by (6) corresponds to the interconnected analog module array architecture shown in Fig. 5, where each analog module employs scaling, summing, and all-pass filtering as building blocks. Continuous-time domain 2-D input signal from the ULA $w(n_x, ct)$ is first processed by the network-resonant 2-D IIR analog filter, which subsequently feeds the time-delay-sum beamformer described by (7). Note that the 1-D low-pass filtering operation present in (8) is moved to the output of the time-delay-sum beamformer as shown in Fig. 5.

Introduction of the network-resonant 2-D IIR pre-filter improves the side-lobe performance in the array pattern at the cost of marginal increase in analog processing complexity. For a ULA of N antennas, the complete SFG in Fig. 5 use $N + \frac{N}{2}(N-1)M$ first-order all-pass filters, $3N$ scaling operations, and $5N-1$ summing operations in total. Note that, for the network-resonant 2-D IIR beam filter, electronic beam steering is achieved by varying the scaling coefficients b_{01}, b_{10}, and b_{11} inside each analog module, whereas the all-pass filters are kept at constant group delay parameter T, which determines the maximum operational frequency of the beam filter. For the subsequent time-delay-sum beamforming section, electronic beam steering is achieved by changing the all-pass filter group delay parameter τ, thereby requiring all-pass filters with tunable group delays.

Frequency response and array pattern simulations can be used to observe the effect of 2-D IIR analog beam pre-filter. Fig. 6(a) shows an example 2-D magnitude frequency response obtained by setting $z_x = e^{j\omega_x}$ and $s_{ct} = j\omega_{ct}$ in (8) for beam direction $\psi = 10°$. Corresponding array pattern is shown in Fig. 6(b) depicting the reduced side-lobe levels, while maintaining the same main-beam selectivity. Projected improvement in interference rejection has been verified in terms of SIR in [13]. For example, with a ULA of 64 elements, desired beam direction $10°$ and interference at $-60°$ from array broadside direction, a relative improvement of 7 dB in SIR has been reported compared to conventional time-delay-sum beamforming [13].

$$G\left(z_x, s_{ct}\right) = \frac{\left[\frac{1}{N}\sum_{n=0}^{N-1}\alpha_n z_x^{-n}\left[\frac{1-\left(\frac{s_{ct}c\tau}{2M}\right)}{1+\left(\frac{s_{ct}c\tau}{2M}\right)}\right]^{Mn}\right]\left[1+z_x^{-1}\right]}{1+\left[b_{10}+b_{11}\left[\frac{1-\left(\frac{s_{ct}cT}{2}\right)}{1+\left(\frac{s_{ct}cT}{2}\right)}\right]\right]z_x^{-1}+b_{01}\left[\frac{1-\left(\frac{s_{ct}cT}{2}\right)}{1+\left(\frac{s_{ct}cT}{2}\right)}\right]}\left[\frac{2}{1+s_{ct}cT/2}\right] \tag{8}$$

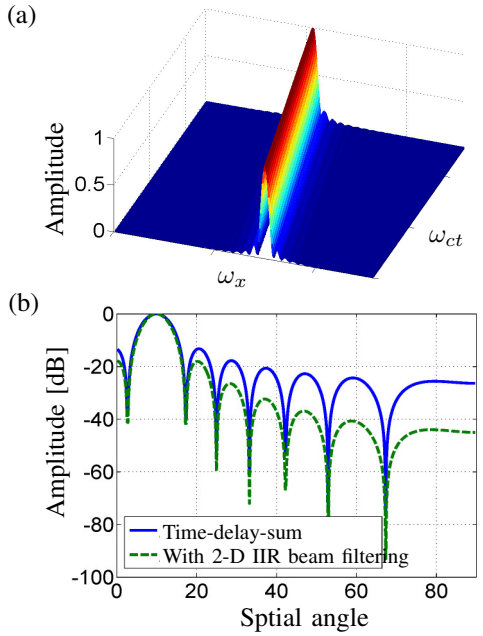

Fig. 6: Example (a) 2-D magnitude frequency response and (b) array pattern corresponding to $G\left(z_x, s_{ct}\right)$ in (8) showing the improved directivity (i.e. reduced side-lobes) due to network-resonant 2-D IIR pre-filtering.

V. Conclusions

We reviewed recent advancements in MD signal processing for directional antenna arrays with improved interference rejection capabilities. Conventional array processing based on zero-manifold-only array transfer functions are reviewed. Network-resonant MD spatio-temporal filters having infinite impulse responses were used in conjunction with conventional phased/timed arrays to obtain enhanced spatial selectivity. Signal processing models for both digital and analog domain implementation of network-resonant 2-D beam filters were described. Inherent multi-input-multi-output analog/digital array processing architectures of the network-resonant 2-D beam filters were employed as a pre-filtering stage to existing phased/timed arrays to obtain improved directivity via reduced side-lobes. Example frequency response and array pattern simulations were provided. Generally speaking, the pre-filtering of a traditional/available phased-/time-array beamformer using a suitable 2-D IIR beam filter can be expected to improve beam directivity by 2-5 dB for the first side lobe, and more than 10 dB in the deep stopband region, without having to increase the number of antennas in the array.

Acknowledgment

This work has been supported by the Office of Naval Research (ONR) grants #N000141310079 and #N000141410197, the US National Science Foundation (NSF) grants #1247940 and #1408361. Dr. Madanayake deeply thanks Dr. Santanu Das (ONR) and Dr. George Haddad (NSF) for their support.

References

[1] W. Liu and S. Weiss, *Wideband Beamforming Concepts and Techniques*. John Wiley and Sons, 2010, ISBN 978-0-470-71392-1.

[2] H. Krishnaswamy and H. Hashemi, "A 4-channel 4-beam 24-to-26GHz spatio-temporal RAKE radar transceiver in 90nm CMOS for vehicular radar applications," in *Proc. IEEE Intl. Solid-State Circuits Conf. Digest of Technical Papers (ISSCC)*, Feb. 2010, pp. 214 –215.

[3] S. Bosse, S. Barth, S. Torchinsky, and B. Da Silva, "Beamformer ASIC in UHFL band for the square kilometer array international project," in *Proc. European Microwave Integrated Circuits Conf. (EuMIC)*, 2010.

[4] M. Elmer, B. D. Jeffs, K. F. Warnick, J. R. Fisher, and R. D. Norrod, "Beamformer design methods for radio astronomical phased array feeds," *IEEE Trans. on Antennas and Propagation*, vol. 60, no. 2, pp. 903–914, 2012.

[5] K. F. Warnick, B. D. Jeffs, J. Landon, J. Waldron, D. Jones, J. R. Fisher, and R. Norrod, "Beamforming and imaging with the BYU/NRAO l-band 19-element phased array feed," in *Proc. 13th Intl. Symp. on Antenna Technology and Applied Electromagnetics and the Canadian Radio Science Meeting ANTEM/URSI*, 2009, pp. 1–4.

[6] C. Fulton and W. Chappell, "Low-cost, panelized digital array radar antennas," in *Proc. IEEE Intl. Conf. on Microwaves, Communications, Antennas and Electronic Systems, COMCAS*, 2008.

[7] L. C. Godara, "Application of antenna arrays to mobile communications II. beam-forming and direction-of-arrival considerations," *Proceedings of the IEEE*, vol. 85, no. 8, pp. 1195–1245, 1997.

[8] G. Zheng, S. Ma, K. kit Wong, and T.-S. Ng, "Robust beamforming in cognitive radio," *IEEE Trans. on Wireless Communications*, vol. 9, no. 2, pp. 570–576, 2010.

[9] A. Van, Ardenne, J. D. Bregman, W. A. Van, Cappellen, G. W. Kant, and J. G. B. De Vaate, "Extending the field of view with phased array techniques: Results of european SKA research," *Proceedings of the IEEE*, vol. 97, no. 8, pp. 1531–1542, Aug. 2009.

[10] L. T. Bruton and N. R. Bartley, "Three-dimensional image processing using the concept of network resonance," *IEEE Trans. on Circuits and Systems*, vol. 32, no. 7, pp. 664–672, July 1985.

[11] D. Dudgeon and R. Mersereau, *Multidimensional Digital Signal Processing*. Prentice-Hall, 1990 ISBN 978-0132276382.

[12] A. Madanayake, C. Wijenayake, S. Wijayaratna, R. Acosta, and S. I. Hariharan, "2-D-IIR time-delay-sum linear aperture arrays," *IEEE Antennas and Wireless Propagation Letters*, vol. 13, pp. 591 – 594, 2014.

[13] C. Wijenayake, A. Madanayake, L. Belostotski, Y. Xu, and L. Bruton, "All-pass filter-based 2-D IIR filter-enhanced beamformers for AESA receivers," *IEEE Trans. on Circuits and Systems I: Regular Papers*, vol. 61, no. 5, pp. 1331–1342, May 2014.

[14] A. Madanayake, S. Wijayaratna, and C. Wijenayake, "Combined time-delay FIR and 2-D IIR filters for EARS, radar, and imaging applications," in *Proc. 57th IEEE International Midwest Symposium on Circuits and Systems (MWSCAS)*, 2014.

[15] A. Madanayak, C. Wijenayake, and L. Belostotski, "Continuous-time 2D IIR + time-delay linear aperture arrays," in *Proc. IEEE Radio Wireless Week*, 2015.

[16] C. Wijenayake, A. Madanayake, and L. T. Bruton, "Broadband multiple cone-beam 3-D IIR digital filters applied to planar dense aperture arrays," *IEEE Trans. on Antennas and Propagation*, vol. 60, pp. 5136 – 5146, 2012.

[17] P. Agathoklis and L. T. Bruton, "Practical-BIBO stability of n-dimensional discrete systems," *IEE Proceedings G on Electronic Circuits and Systems*, vol. 130, no. 6, pp. 236–242, Dec. 1983.

[18] A. Madanayake and L. Bruton, "A speed-optimized systolic-array processor architecture for spatio-temporal 2D IIR broadband beam filters," *IEEE Trans. on Circuits and Systems-I: Regular Papers*, vol. 55, pp. 1953–1966, 2008.